OS
no actions
asb
ostk

OFFICE OF CONTRACT ADMINISTRATION

Termination of Delivery Order under E-21-A00

Date: 2/2/78

Project Title: Task HR-07 under NCSL Onmibus R&D Program

Project No: E-21-A07 & E-19-A01 (Co-Projects)

Contract No: N61339-75-C-0122; Delivery Order No: HR-07

Project Director: Dr. Joy (EE) and Dr. Hochman (ChE)

Sponsor: Naval Coastal Systems Laboratory; Panama City, FL 32407

Effective Termination Date: 9/30/76

TERMINATED

Delivery Order Closeout Actions Remaining:

X Final Invoice

X Final Report of Inventions

___ Government Property Inventory and Related Certificate - 14 Oct '77

___ Classified Material Certificate 6 Sept '77

Assigned to: School of Electrical Engineering & Chemical Engineering

Copies to:

Project Director (2)
School Director (2)
Dean
Accounting Office
Procurement Office
Security Coordinator (OCA)
Reports Coordinator (OCA)
Project File (OCA) (2)
Other _____

NOTE: SINCE AN INITIATION SHEET WAS NOT ISSUED ON THIS PROJECT (A DELIVERY ORDER UNDER E-21-A00), THIS SHEET IS BEING ISSUED TO TERMINATE THE PROJECT.

CONTINUED AS E-21-A18 and E-19-A02

GEORGIA INSTITUTE OF TECHNOLOGY
SCHOOL OF ELECTRICAL ENGINEERING
ATLANTA, GEORGIA 30332

TELEPHONE: (404) 894-2901

6 April 1976

Naval Coastal Systems Laboratory
Attn: Mr. Max Weber
Minesweeping Division - Code 721
Panama City, Florida 32401

Subject: Monthly Letter Report No. 1, Task HR-07 under NCSL Omnibus R&D Program Contract N61339-75-C-0122, "A High Current Minesweeping Electrode Investigation" covering the period 9 March 1976 to 31 March 1976.

Gentlemen:

The start-up phase of this program has been completed. The start-up phases included study of reports, papers and books concerning the development of the existing electrodes. It also included inspection of electrodes before and after normal use and inspection of the NCSL facilities for remanufacture of electrodes. This phase resulted in the identification of three areas of preliminary investigation:

1. Aluminum Electrodes;
2. Noble Metal Electrodes;
3. Carbon/Graphite Electrodes.

A key electrical parameter basic to all three areas of preliminary research is the current distribution on the electrodes. Investigation has begun to use existing computer programs to display the electrode current distributions as a function of electrode size, spacing, and conductivity.

Chemical analysis has also begun on the fouled cathode electrode samples to identify cathode compounds.

The cumulative man-hours expended is 329 and the expended funds total approximately $6733.

Respectfully submitted,

Edward B. Joy
Project Director

gc

cc: Dr. R. F. Hochman
Dr. D. T. Paris

E-21-A07

A HIGH-CURRENT MINESWEEPING ELECTRODE INVESTIGATION

By

E. B. Joy, G. K. Huddleston, and W. M. Leach
School of Electrical Engineering

And

R. F. Hochman, J. G. Rinker, M. Marek, and K. J. Bundy
Metallurgy Department, School of Chemical Engineering

GEORGIA INSTITUTE OF TECHNOLOGY
Atlanta, Georgia

FINAL RESEARCH REPORT
TASK HR-07
CONTRACT N61339-75-C-0122
9 March 1976 – 30 June 1976

1976

Prepared for
NAVAL COASTAL SYSTEMS LABORATORY
MINESWEEPING DIVISION
PANAMA CITY, FLORIDA 32401

A HIGH-CURRENT MINESWEEPING ELECTRODE INVESTIGATION

by

E. B. Joy, G. K. Huddleston, and W. M. Leach
School of Electrical Engineering

and

R. F. Hochman, J. G. Rinker, M. Marek, and K. J. Bundy
Metallurgy Department
School of Chemical Engineering

Georgia Institute of Technology
Atlanta, Georgia 30332

June 1976

FOREWORD

This final report was prepared by the School of Electrical Engineering and the Metallurgy Department of the School of Chemical Engineering, Georgia Institute of Technology, Atlanta, Georgia 30332 in fulfillment of the requirements of Task HR-07 under NCSL Omnibus R&D Program Contract N61339-75-C-0122 for the Naval Coastal Systems Laboratory, Panama City, Florida.

The period of performance covered by Task HR-07 and this report is 6 March 1976 to 30 June 1976.

Report authors are E. B. Joy, G. K. Huddleston, and W. M. Leach from the School of Electrical Engineering and R. F. Hochman, J. G. Rinker, M. Marek, and K. J. Bundy from the Metallurgy Department of the School of Chemical Engineering.

The authors acknowledge the expert assistance of Mr. Miller Epps and Mr. Max Weber of the Naval Coastal Systems Laboratory in providing operational and historical insight concerning the minesweeping problem and for their guidance and concern.

The views and conclusions contained in this document are those of the authors and should not be interpreted as necessarily representing the official policies, either expressed or implied, of the Naval Coastal Systems Laboratory or the U.S. Government.

TABLE OF CONTENTS

LIST OF ILLUSTRATIONS

LIST OF TABLES

CHAPTER 1

INTRODUCTION

This report documents the efforts and results of an investigation of high-current minesweeping electrodes. The purpose of this investigation was to reexamine the design and selection of high-current minesweeping electrode materials in an attempt to realize a long-life, cost-effective electrode. It was hoped that a new look by electrochemical and electromagnetic engineers working together might uncover a new material or improve significantly an old concept for application to the high-current electrode problem.

A literature search was performed to understand the previous results and conclusions by other investigators who had designed and experimented with previous electrode materials. The literature in this highly specialized subject area consists primarily of Naval Coastal System Laboratory reports and Aero-jet-General Corporation reports. A few papers in electrochemistry journals were found but none related to high current. Both the Bell System and the Institute of Electronic and Electrical Engineering Society on Power Apparatus and Systems are concerned with electrochemical corrosion of bare conductors in the ground and in salt marshes; however, they are not concerned with high current flow. Interestingly, the power community and power cable manufacturers, such as General Cable Company, are interested in high current flow into the ground (or sea) but not as normal operation. They are concerned when a fault (short circuit)

condition occurs and the outer bare metallic conductor has been corroded open and forces high current to flow from the metallic outer conductor into the ground. In the fault condition, however, personnel safety and not the lifetime of the conductor are of concern. In both cases, the primary goal is the reduction of electrochemical corrosion of base conductors.

Two books were also useful in this investigation; the first was Earth Resistances by Tagg and the second was Earth Conduction Effects in Transmission Systems by Sunde. Both books describe methods of electromagnetic analysis for conductors in a conducting medium.

The Georgia Tech investigation team made an on-site inspection of the Naval Coastal Systems Laboratory minesweeping facilities and learned many aspects of the operational problems associated with existing aluminum high-current minesweeping electrodes. The team inspected actual minesweeping electrodes including new, remanufactured and fully used electrodes. From the fully used electrodes, samples were taken of aluminum strands from anode and cathode electrodes for electrochemical analysis. Chapter 3 reports on the findings of these analyses.

Approximately midway through this four-month investigation, the investigation team met to consolidate the research effort and make a preliminary selection of electrode materials for more indepth analysis. The preliminary efforts indicated that only three electrode concepts were viable for long life operation: (1) some form of graphite (a conducting non-corrosive, non-metal); (2) a noble metal (a non-corrosive metal, either pure metal or as a plating on another metal); and (3) aluminum (the best of the corrosive metals). The

experience with graphite and carbon mixtures by both the Bureau of Ships and Aeroject-General showed that there was hope for some form of graphite; however, either due to lack of mechanical strength or early failures with laboratory samples, graphite was rejected. Chapter 6 reports on a new graphite electrode. Noble metal electrodes had likewise been proposed in the past; however, the cost of a pure noble metal electrode was prohibitive compared to the then inexpensive aluminum electrodes. Noble metal plating was not seriously considered in earlier work as noble metal plating techniques are only now becoming commerically developed. Chapter 7 reports on a new noble metal electrode concept. Aluminum was retained as a possibility in the hope that new electrode shapes or method of operation could be discovered to increase the aluminum electrode lifetime. Chapter 3 gives an indepth analysis of the aluminum electrode.

The next phase of this investigation focused on analysis of the minesweeping electrode system. The various aspects of the system were analyzed and included: the analysis of the electrode current distribution which is reported on in Chapter 4; the analysis of the magnetic field strength of the electrode system, which is reported on in Chapter 5; the electrochemical analysis of the aluminum dissalution process which is reported on in Chapter 3; the electrical analysis of the electrode system which is reported on in Chapter 2.

Chapter 8 reports on the conclusions of this investigation and recommends the next steps to be taken in the development of a high-current, long-life, cost-effective minesweeping electrode.

CHAPTER 2

ELECTRODE SYSTEM ELECTRICAL ANALYSIS

The electrical circuit of the high-current magnetic minesweeping electrode system for dc is composed of four resistors in series. The four resistors are: (1) the internal resistance of the anode electrode; (2) the sea water path resistance between the two electrodes; (3) the internal resistance of the cathode electrode; and (4) the internal resistance of the S-cable. These four resistances cannot be physically separated in the above manner; however, it has been found that this simple model is adequate for estimating total circuit resistances. The total circuit resistance, together with the desired current amplitude specify the total power requirement of the minesweeping system generator. It is clear, therefore, that absolute minimum resistance is desirable.

The internal resistance of the S-cable is the easiest resistance to estimate and will be discussed first. The resistance of any cable which has a uniform conductor crossectional area and for which the total current flows an entire length L is given by the following equation:

$$R_{S\text{-cable}} = \frac{L}{A} \frac{1 + .0056(t - 20°)}{\sigma_{20}} \qquad (2\text{-}1)$$

where σ_{20} is the conductivity of the metal specified at 20°C, which for hard-drawn aluminum is equal to 3.536×10^7 mhos/meter, and t is the temperature (°C) of the conductor. The temperature of the S-cable must be calculated from a thermodynamic analysis. Existing S-cables

have been found to reach temperatures near 100°C and are usually limited to this value due to temperature limitations of cable constituant materials.

The resistance of the anode and cathode electrodes is very difficult to determine since the current distribution within the electrodes is not known. All equations developed to date for the current distribution predict zero current density at the aft end of each electrode. Examination of used electrodes, however, reveals that the fore and aft ends of both anode and cathodes are the points of maximum current density for the electrodes. Thus, the determination of electrode resistances is truly an estimate. The estimate is based on the use of the S-cable resistance equation. The electrode resistance is calculated as if it were an S-cable and then modified by a correction factor for non-constant current flow. The correction factor must always be less than one since all the current does not flow through the resistance of the electrode due to conduction into the sea. A correction factor of 0.5 is commonly used. As will be shown later, the electrode resistances are usually less than the S-cable resistance and much less than the sea water path resistance; hence, the inaccuracy of the electrode resistance calculation is not normally significant in the total resistance estimate.

The sea water path resistance is given for the case of two perfectly conducting cylindrical electrodes of length L and diameter D lying along a line parallel to the sea surface submerged at a depth Z and separated by a distance X (head to tail separation) as:

$$R_{sea} = \frac{1}{\sigma \pi L} \ell n\left(\frac{2L}{D}\right) - \frac{1}{2} \ell n\left(1 + \frac{\ell}{X}\right) + \frac{1}{2} \ell n \frac{\sqrt{1+B^2} + 1}{\sqrt{1+B^2} - 1} \qquad (2.2)$$

where σ is the conductibility of the sea water and

$$B = \frac{4Z - D}{L} \qquad (2.3)$$

The above equation for the sea water path resistance assumes an infinite depth sea. Measurements have revealed that the resistance calculated with the above equation may increase or decrease by as much as 25% due to a sea depth of 40 feet, depending on the conductivity of the sea bottom. The equation does not take into effect the non-uniform current distribution on the electrode which may be significantly different that the postulated distribution. However, measured results with aluminum electrodes are in close agreement with this equation. It is important to understand the change in this resistance for variations in the equation parameters as in practice, this resistance is the dominate and controlling resistance in the electrode system. To achieve lower system resistance, the electrode length should be increased, the electrode diameter should be increased, the separation between electrodes should be decreased and/or the submergence should be increased. Increasing the length of the electrode increases hydrodynamic drag linearly. Increasing diameter also increases electrode drag but at a rate greater than linearly. Decreasing electrode separation results in a smaller area of magnetic field penetration and defeats the purpose of the open loop system. Increasing submergence (placing the electrode at greater depth) increases the drag of the system in a manner which depends on the method of submergence. The submergence factor however,

is a large factor resulting in an increase of 2.0 when the electrode is floating with only one half of the electrode submerged. At approximately 10 feet of depth, almost 80% of infinite submergence benefits are realized.

Altogether, these factors result in the conclusion that the outer surface area of the electrode controls the sea water path resistance and at the same time controls the drag of the electrodes. Likewise, submergence lowers resistance, but increases drag. Thus the inevitable trade-off between higher resistance (requiring more power generation) and higher drag (requiring more towing capacity) arises. The sea water path resistance also dictates for existing and planned power generation and towing capacities, the outer surface area of the electrodes, no matter what the composition of the electrodes, is basically fixed. No large changes in the surface area of the electrodes is feasible under present specifications of the minesweeping systems under consideration. To illustrate the relative values of the four circuit resistances, Figure 2-1 gives the calculated resistances for the existing PE-3 electrode. This figure also reiterates the trade-off between generator capacity and hydrodynamic drag.

ELECTRODE SIZE

1. CIRCUIT RESISTANCE (EXAMPLE: PE-3)

   R_{SEA} = .0212 Ω

   $R_{ELECTRODE}$ = .0016 Ω (2 OF THESE)

   R_S = .008 Ω

   R_{TOTAL} = .0324 Ω

2. R_{SEA} IS THE DOMINATE RESISTANCE AND IS SHOWN TO BE PRIMARILY DEPENDENT ON THE ELECTRODE SURFACE AREA.

3. DRAG IS ALSO PRIMARILY DEPENDENT ON THE ELECTRODE SURFACE AREA.

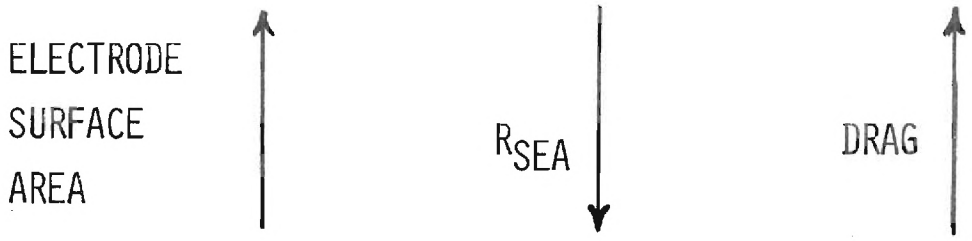

CONCLUSION

AS GENERATOR IS ALREADY FIXED+TOTAL DRAG IS ALREADY TOO LARGE;
ELECTRODE SIZE MUST REMAIN FIXED AT PRESENT SIZE.

Figure 2-1. PE-3 Electrode Resistances

CHAPTER 3

ALUMINUM ELECTRODES

3.1 Introduction

Aluminum has been used in electrodes for minesweeping systems, and is still used today in the PE-3 electrode. This metal has been found to be acceptable for this application due to its combination of good electrical conductivity, relatively low specific gravity, adequate mechanical properties, good corrosion resistance (due to its high +3 valence state), and low cost when compared to other alternative metals. However, future systems must have the capability to operate at higher current levels than have been previously utilized, and so it is important to re-examine aluminum and other possible choices with respect to their suitability for these new systems. The following report summarizes the work to date in the evaluation of aluminum as a possible anode and cathode material.

3.2 Aluminum As An Anode Material

Two types of configurations for the anode to be used in a high performance magnetic mine sweeping system were considered and compared with respect to their resistance to dissolution. Configuration 1 consists of a hollow tube and Configuration 2 consists of wires surrounding a core of bouyant material as shown in Figure 3-1. The outside diameter, denoted by D_0, in both cases was assumed to be 3.5 inches.

Configuration 1:

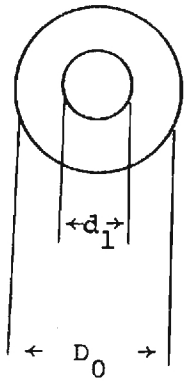

D_0 = 3.5 inches

Configuration 2:

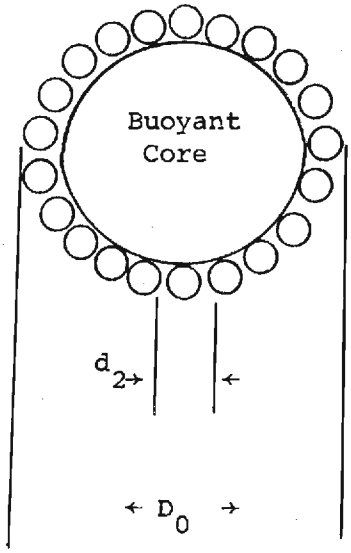

D_0 = 3.5 inches

FIGURE 3-1. Aluminum Electrode Configurations.

Corrosion Resistance of Configuration 1

The inside diameters of Configuration 1 (tubes), denoted by d_1, required to retain 50% of the original thickness after 24 hours and 48 hours of exposure to the corrosive environment were calculated on the basis of Faraday's law:

$$W = k \int_0^{t'} I dt$$

where W is the weight loss of metal in time t', I is the total current, which is a function of time in the general case, and k is a constant factor called the electrochemical equivalent which, for aluminum, equals 0.96×10^{-4} grams per coulomb.

Four values of current density (at time, t, equal to zero) were used in these calculations: 0.4, 0.83, 1.2, and 1.5 amp/in^2. For each current density, d_1 was determined for two sets of conditions: (1) total current remaining constant with time, and (2) current density remaining constant. From consideration of Faraday's law and the geometry of Configuration 1, the following equations were derived from which d_1 can be determined for the operating conditions, times and current densities of interest:

Constant current:

$$kj_0 D_0 t' = \frac{\rho}{16} (3D_0^2 - 2d_1 D_0 - d_1^2)$$

Constant current density:

$$kj_0 (D_0 t' - \frac{kj_0 t'^2}{\rho}) = \frac{\rho}{16} (3D_0^2 - 2d_1 D_0 - d_1^2)$$

where: 1) ρ is the density of aluminum; 2) $j_0=I_0/A_0$ where I_0 is the total current flowing at time zero and $A_0=\pi D_0 L$, the surface area of a cylinder of diameter D_0 and length L.

From the values of d_1 and D_0, specific gravities of the hollow tube assemblies were calculated so as to identify which of the anodes would be buoyant. Of those inside-outside diameter combinations which were sub-buoyant, further calculations were performed to see whether or not any of these would be submerged at depths between 10 and 20 feet with no restraint at one end of the anode and towing speeds of 5 and 15 knots. The calculations for sub-buoyant structures are discussed in further detail in Appendix A.

The results of the analysis described in this section is given in Table 3-1.

In Table 3-1 the anodes which would be bouyant are denoted by (b). The results summarized in this table indicate that for Configuration 1, 50% of the wall thickness can be retained in a bouyant tube after 24 hours at current densities of 0.4 and 0.83 amps/in^2, but that for current densities of 1.2 and 1.5 amps/in^2 the tubes would not be bouyant. The only possible useful sub-bouyant anode found, denoted by (sb) in Table 1, was one which would be submerged between 1 and 20 feet when operating under conditions of a constant current density of 1.2 amps/in^2 at a towing speed of 15 knots. For 50% of the wall thickness to be retained after 48 hours of operation, a bouyant anode could be used at 0.4 amps/in^2, but not at 0.83, 1.2, or 1.5 amps/in^2.

Table 3-1

Tube Inside Diameters Necessary to Retain 50% of Dimensions after 24 and 48 Hours at Various Current Densities and Operating Conditions for Configuration 1 and the Specific Gravities, SG, of Such Assemblies.

t' = 24 hours

j_0 (amps/in^2)	Constant Current		Constant Current Density	
	d_1 (inches)	SG	d_1 (inches)	SG
0.40	3.193	0.453 (b)	3.200	0.443 (b)
0.83	2.847	0.914 (b)	2.878	0.874 (b)
1.20	2.533	1.286	2.600	1.210 (sb)
1.50	2.267	1.567	2.375	1.457

t' = 48 hours

j_0 (amps/in^2)	Constant Current		Constant Current Density	
	d_1 (inches)	SG	d_1 (inches)	SG
0.40	2.872	0.882 (b)	2.900	0.846 (b)
0.83	2.119	1.710	2.255	1.579
1.20	1.379	2.281	1.700	2.063
1.50	0.684	2.597	1.250	2.356

Configuration 1 - Mechanical Considerations

In the case of the hollow tubes (Configuration 1) a strength of materials type stress analysis indicates that, in addition to the difficulty in obtaining bouyant anodes at the higher current densities, another possible problem with aluminum anodes could be high stress levels under certain conditions. When a sea state 4 condition is present, at certain moments a 150-foot anode would be suspended at the ends of the crests of the waves and would be bending under its own weight as a simply supported beam. Under these conditions, the maximum tensile stress occurs at the center of the span and is given by the following equation:

$$|\tau_{xx}|^{max} = \frac{M_x^{max} y}{I_{zz}}$$

where $|\tau_{xx}|^{max}$ is the maximum absolute value of the axial tensile stress, y is the corresponding distance from the neutral axis, I_{zz} is the second moment of area of the cross-section, and M_x^{max} is the maximum bending moment.

For a tube length L, outside diameter D_0, and inside diameter d_1:

$$y = D_0/2$$

$$I_{zz} = \frac{\pi}{64} (D_0^4 - d_1^4)$$

$$M_x^{max} = \frac{WL^2}{8} \text{ (at the center of the span}$$

where W is the uniform load present per unit length due to the weight of the beam.

The maximum tensile stress was calculated for a tube of 3.5 inches OD and 2.8 inches ID (which are roughly the dimensions of a tube which would retain 50% thickness after 24 hours for a current density j_0 = 0.83 amps/in^2 and 150 feet in length). In this case, the maximum stress at the center of the span is in the neighborhood of 50,000 psi. In order to reduce the stress levels either a sub-bouyant anode could be used, bouyant sections could be linked together in, say, 25 foot lengths, or a flexible cable such as Configuration 2 could be employed.

Corrosion Resistance of Configuration 2

An analysis similar to that given previously for Configuration 1 was carried out for Configuration 2 (wires surrounding a core of bouyant materials). Wire diameters, denoted by d_2, were calculated which would retain 50% of the diamter after 24 and 48 hours. The current densities at t=0 used were the same as before numerically, but were considered to be apparent current densities (i.e., total current divided by the surface area of a tube 3.5 inches in diameter), and are denoted as j_0^{app} in this section. d_2 values were calculated for three sets of operating conditions: (1) constant current, (2) constant apparent current density, and (3) constant true current density (total current divided by instantaneous total surface area of the wires).

As before, Faraday's law and the geometry of the system were used to derive equations which express the dimension of interest, which is d_2 here, in terms of current density and dissolution time for the various operating conditions. These equations are given below:

Constant current:

$$kj_0^{app} D_0 t' = \frac{3\rho}{16} \cdot N d_2^2$$

Constant true current density:

$$kj_0^{app} \left(D_0 t' - \frac{kj_0^{app} D_0^2 t'^2}{\rho N d_2^2}\right) = \frac{3\rho}{16} \cdot N d_2^2$$

Constant apparent current density:

$$\frac{8kj_0^{app} t'}{N\rho} = d_2 + (D_0 - 2d_2) \cdot \ln\left(\frac{D_0 - d_2}{D_0}\right)$$

All the quantities in these equations have been previously defined except for N, which is the number of wires which surround the central core of buoyant material:

$$N = \frac{\pi}{\tan^{-1}\left(\frac{d_2}{D_0 - d_2}\right)}$$

From the values of d_2 and D_0, the specific gravities of the core required to make anodes of Configuration 2 be buoyant (specific gravity of the whole assembly equal to 0.97) were then determined. For those structures which could not be made buoyant, the possibility that cores could be found which would produce an anode submerged 10 feet or 20 feet at speeds of 5 and 15 knots was also examined.

The data obtained from these calculations are given in Table 3-2.

TABLE 3-2

Wire Diameters Necessary To Retain 50% of Thickness After 24 and 48 Hours For Various Operating Conditions and Current Densities with Configuration 2 and the Corresponding Specific Gravities of the Core Material, SG_{core}.

t' = 24 hours

j_0^{app} (amps/in^2)	Constant Current		Constant True Current Density		Constant Apparent Current Density	
	d_2(in.)	SG_{core}	d_2(in.)	SG_{core}	d_2(in.)	SG_{core}
0.40	0.13	0.743	0.10	0.800	0.13	0.743
0.83	0.29	0.375	0.21	0.574	0.27	0.428
1.20	0.43	*	0.31	0.320	0.41	*0.006
1.50	0.56	----	0.40	*0.040	0.52	*

t' = 48 hours

j_0^{app} (amps/in^2)	Constant Current		Constant True Current Density		Constant Apparent Current Density	
	d_2(in.)	SG_{core}	d_2(in.)	SG_{core}	d_2(in.)	SG_{core}
0.40	0.28	0.402	0.20	0.596	0.27	0.428
0.83	0.64	----	0.45	*	0.58	----
1.20	1.02	----	0.70	----	0.87	----
1.50	1.41	----	0.94	----	1.11	----

Explanation of symbols in Table 3-2: If there is a specific gravity of the core material below which the specific gravity of Configuration 2 assemblies as a whole would be buoyant (considered to be an SG of 0.97), it is given as a number in the SG_{core} column. Those wire diameters for which the SG_{core} column is marked with a blank, (----), correspond to those assemblies which would be submerged in more than 20 feet of water at speeds of 15 knots or less regardless of what the specific gravity of the core is. Those assemblies marked with an asterisk are those which would be submerged in 10 feet or 20 feet of water when the tow speed is 5 knots or 15 knots. The quantitative data concerning the specific gravities required are given in Appendix A.

By comparing Tables 3-2 and 3-2 it can be seen that the levels of current density which allow retention of 50% of the dimensions after 24 and 48 hours are basically similar for the two geometrical configurations, although the situation is improved slightly for Configuration 2.

To retain 50% of the wire diameter after 24 hours and still have a buoyant anode with a core of a practical specific gravity, say 0.3 and above, apparent current densities at t=0 of 0.4 and 0.83 amps/in^2 could be used for all three types of operating conditions. Also, at 1.2 amps/in^2 a buoyant assembly could be obtained under constant true current density conditions and sub-buoyant assemblies submerged 20 feet at 15 knots could be obtained (with practical core specific gravities) under conditions of constant current and constant apparent current density (see Appendix A). To retain 50% of the wire diameter after 48 hours, an apparent current density of 0.4 amps/in^2 could be used in anodes which would be buoyant. For the higher current densities,

however, the only possibly useful sub-buoyant assembly would be one operating under constant true current density conditions and submerged 20 feet at 15 knots. This anode could only be used at an apparent current density at t=0 of .83 amps/in^2 (see Appendix A).

3.3 Cathode Fouling

The fouling on standard PE3 cathodes was found to be a scale-like deposit containing $Al(OH)_3$ and $Al_2O_3 \cdot 3H_2O$, with significant amounts of Mg, Ca, Cu, and Si. The formation of this deposit is obviously a complex process, but the primary factor is the oxygen reduction reaction:

$$O_2 + 2H_2O + 4\bar{e} \rightarrow 4OH^-$$

The predominance of oxygen reduction as the cathodic half cell reaction leads to a high concentration of OH^- ions near the surface of the cathode. There are several consequences of this:

1. The pH in the boundary layer rises to a value at which aluminum is susceptible to corrosion.
2. Mg^{++} (and other cations present in seawater) migrates to the cathode and combines with OH^- to form $Mg(OH)_2$, which is very insoluble and precipitates in the vicinity of the cathode surface.
3. The corrosion products of the aluminum, $Al(OH)_3$ and $Al_2O_3 \cdot 3H_2O$, probably trap $Mg(OH)_2$ and other cation salts in the fouling layer.

Table 3-3 summarizes the results of election diffraction and microprobe analysis of the cathodic deposits. Aluminum and magnesium hydroxides were estimated to comprise 40 to 50% of the deposit, with various minor constituents totaling about 10 to 15%, and the remainder being hydrated aluminum oxide.

Theoretically, if all cathodic reactions produced gaseous or soluble products, there would be no fouling. Since aluminum suffers cathodic corrosion which has insoluble products, fouling will always occur on aluminum cathodes. For platinum, the exchange current density for the hydrogen electrode is eight orders of magnitude higher than that for aluminum; hence, it is possible that hydrogen evolution may be an important cathodic reaction for platinum. This is significant not only because the reaction product is gaseous, but also because the bubbling action might disperse precipitating cation salts such as $Mg(OH)_2$.

Even if some scale formation does occur, it is possible that it could be removed by periodic polarity reversals of the electrodes. The critical parameters in this process would be the basic effectiveness of the reversal in expelling the fouling, the time limits on the intervals between reversals and the time limits on the anodic descaling of the cathode. For any electrode these times would have to be less than or equal to the time of a single sweep and the descaling time would have to be less than or equal to the turnaround time between sweeps.

The cathodic samples examined had suffered a weight loss of about 21% in approximately 60 hours of operation. This data may be used in calculating the maximum useful life of an aluminum cathode

TABLE 3-3

ANALYSIS OF CATHODIC DEPOSITS

Compounds Identified:

$Al(OH)_3$	$Mg(OH)_2$
$Al_2O_3 \cdot 3H_2O$	(Ca,Al)silicate

Elements Identified:

Significant	Trace
Aluminum	Iron
Magnesium	Chlorine
Calcium	Boron
Copper	Potassium
Silicon	Sodium

which is periodically descaled by current polarity reversals. Assuming that a 15-second reversal done four times per operating hour would be an effective descaling procedure, the projected service life of the cathode would be 180 hours. This calculation assumes uniform weight loss during anodic descaling; the occurrence of pitting might shorten the service life.

CHAPTER 4

ELECTRODE CURRENT DISTRIBUTION

4.1 Introduction

In open-loop minesweeping, current is emitted into the sea water from one electrode and is recovered some distance away by a second electrode. One end of each electrode is connected to one terminal of the electrical power source: (i) the forward electrode is connected to one terminal via a short, insulated service cable; (ii) the aft electrode is connected to the other terminal of the power source via a much longer service cable (S-cable). The electrical resistance presented by the electrodes to the power source is normally on the order of milliohms.

The voltage between the terminals of the power source is normally adjusted to maintain a specified value of current flow between the electrodes. One end of the anode is maintained at $+V_s$ volts; one end of the cathode is maintained at $-V_s$ volts. Current entering the terminal end of the anode is attenuated as it flows down the length of the electrode since a portion of the current flows from the surface of the electrode into the conductive sea water. It is desired to find the distributions of current $I(z)$ inside the electrodes, the distribution of current $i(z)$ leaving/entering the electrodes, and the relative effects of electrode conductivity, sea water conductivity, and other electrode parameters on these current distributions.

Perhaps the most recent derivation of electrode current distribution is given in Appendix B of Reference 1. The current

at any point in the conductor as a function of the distance z from the terminal end is given by

$$I(z) = I_0\left[\frac{\sinh B\ell\cosh Bz - \cosh B\ell\sinh Bz}{\sinh B\ell}\right] \qquad (4\text{-}1)$$

where:

$B = \sqrt{rg}$

r = resistance in the conductor (ohms/unit length)

g = conductivity of the sea water (mhos/unit length)

ℓ = length of the electrode. (4-2)

Equation (4-1) predicts a current I_o entering the electrode at the terminal (excited) end; at the other end of the electrode, $z=\ell$, the current is assumed to be zero. The data of Reference 2 show, however, that the material loss due to electrolytic action is greatest at both ends of the electrode; i.e. these experimental data show that the current leaving the electrode is greatest at the input end, decreases to a minimum at approximately 2/3 the length of the electrode, and then begins to increase again. The analysis leading to Equation (4-1) above shows a monotonically decreasing surface current density i(z) since

$$i(z) = \frac{dI}{dx} \qquad (4\text{-}3)$$

---

[1] Murphy, W. O., Jr. and Walcott, F. J., Jr., "Advanced Magnetic Minesweeping System Investigation Program," AESC Report 3848, November 1969.

[2] Hudson, J. A., "Design Considerations of a Magnetic Minesweeping Cable Assembly for the PAGE System," MDL Report i-63, October 1964.

according to the analysis.

This shortcoming of the analysis is not a major problem in some types of calculations for the open-loop system; however, it is felt that a more accurate model is required for calculations involving electrode electrolysis (as in the case of aluminum electrodes), heating of electrodes (as in the case of the jacketed or graphite electrodes), and in parametric studies aimed at adjusting the current distributions by adjusting electrode parameters. In what follows is a description of a new approach to developing a more accurate model.

4.2 Formulation of the Problem

The electrode geometry of interest is shown in Figure 4-1. The terminal ends of the anode and cathode are maintained at $+V_s$ and $-V_s$ volts as shown and represent the region containing the driving source. In all other (source-free) regions, Maxwell's equations for the time-invariant case are satisfied at every point [3]:

$$\nabla \times \underline{E} = 0 \tag{4-4}$$

$$\nabla \times \underline{H} = \underline{J} \tag{4-5}$$

$$\nabla \cdot \epsilon \underline{E} = 0 \tag{4-6}$$

$$\nabla \cdot \mu \underline{H} = 0 \tag{4-7}$$

where $\underline{E}$ is electric field intensity (V/m), $\underline{H}$ is magnetic field intensity (A/m), $\underline{J}$ is current density (A/m^2), and ϵ and μ are the

[3] D. T. Paris and F. K. Hurd, "Basic Electromagnetic Theory," McGraw-Hill Book Company, New York, 1972.

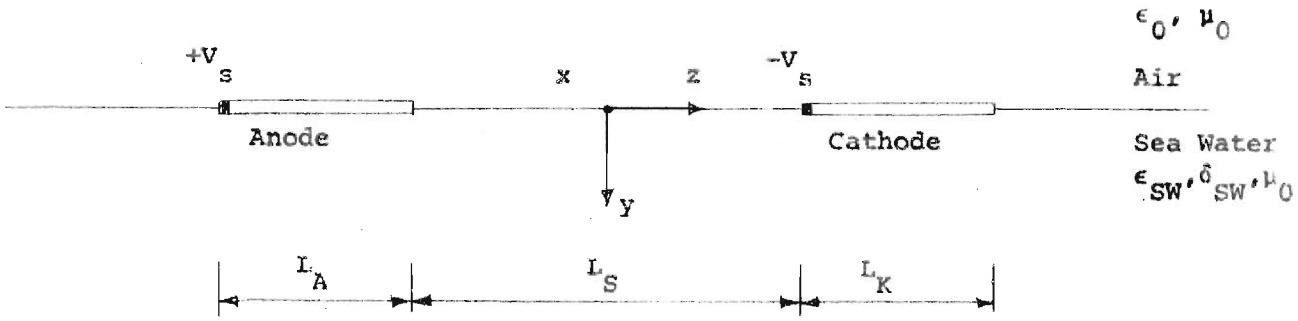

FIGURE 4-1. Electrode Geometry

permittivity and permeability of the medium (air, sea water, or electrode material). Since the curl of the gradient is identically zero, Equation (4-4) implies that $\underline{E}$ may be written as the gradient of a scalar (potential) function ϕ:

$$\underline{E} = -\nabla\phi. \tag{4-8}$$

From Equations (4-6) and (4-8), Laplace's equation follows; viz.,

$$\nabla \cdot \epsilon\underline{E} = \nabla(-\epsilon\nabla\phi) = -\epsilon\nabla^2\phi = 0 \tag{4-9}$$

or

$$\nabla^2\phi = 0 \tag{4-10}$$

where ∇^2 is the Laplacian operator

$$\nabla^2 = \frac{\partial^2}{\partial x^2} + \frac{\partial^2}{\partial y^2} + \frac{\partial^2}{\partial z^2} \tag{4-11}$$

Equation (4-10) indicates that the formal solution of the electrode problem depicted in Figure 4-1 will involve the solution of Laplace's equation subject to the boundary conditions at the interfaces between different media, at infinity, and at boundaries where the potential ϕ is specified. Once the potential $\phi(x,y,z)$ is determined, the current distribution $\underline{J}$ may be obtained directly from the constitutive relation

$$\underline{J} = \sigma\underline{E} = -\sigma\nabla\phi \tag{4-12}$$

where σ is the conductivity (mhos/m) of the medium. The current I along the length of an electrode would then be given by the surface

integral of the z-component of $\underline{J}$ over the cross-section of the electrode. The distribution i of current leaving the electrode would be given similarly by a surface integral of the component of $\underline{J}$ normal to the electrode surface.

The law of conservation of charge can be used to show that Kirchoff's current law and Laplace's equation are equivalent at a point. The law states, for the time-invariant case,

$$\nabla \cdot \underline{J} = 0. \tag{4-13}$$

Substituting Equation (4-12) into the above equation yields

$$\nabla \cdot (\sigma \underline{E}) = \nabla \cdot (-\sigma \nabla \phi) = -\sigma \nabla^2 \phi = 0 \tag{4-14}$$

which is just Laplace's equation. Equations (4-13) and (4-14) indicate that in a source-free, conducting region of Figure 4-1, the potential $\phi(x,y,z)$ will be distributed such that the net current into any closed volume is zero. Furthermore, the satisfaction of Kirchoff's current law at every point in a conducting region is equivalent to solving Laplace's equation. This is an important observation in regard to effecting a numerical solution for the electrode system of Figure 4-1 using a digital computer.

A numerical solution of the electrode problem involves the determination of the potential ϕ at discrete points in the region of Figure 4-1. The accuracy of the solution and the degree of resolution obtained depend on the distance between the discrete points relative to the dimensions of the electrodes and their spacing; i.e., on the number of points. For reasonable accuracies, the number of points required for the three-dimensional geometry may be enormous and the time to effect a solution on a digital computer prohibitive.

It is, therefore, advantageous for practical reasons to reduce the three-dimensional geometry of Figure 4-1 to two dimensions y and z. This has the effect in Figure 4-1 of making the regions have infinite extent in the x-direction so that the potential ϕ is not a function of x. Although there are no guarantees that the two-dimensional solution will yield accurate answers which conform to physical facts, it is expected that this will be the case. The proof of the validity of the solution will lie in the comparisons of theoretical and measured results.

Another practical consideration involved with a numerical solution of even the two-dimensional problem is that of the allowable extent of the region containing the electrodes. Ideally, the region would be of infinite extent, and the potential ϕ would satisfy the boundary condition at infinity. Practically, the extent of the region must be limited so that there will be only a finite number of discrete points at which ϕ must be found.

The method used here to limit the extent of the region is that of imaging and periodicity. The region containing the electrodes in Figure 4-1 is considered to be the object cell. The cells adjacent to each of the four sides are obtained by imaging the object cell about its respective sides. When the image cells are, in turn, imaged about their sides, a periodic structure of cells results and extends to infinity. The imaging of the cells has the effect of preventing the flow of current across the boundary of any cell. Clearly, the larger the object cell, the more closely will the solution conform to the ideal case of a single cell of infinite extent.

As a further simplication of the electrode problem, consider the case of totally submerged electrodes; i.e., in Figure 4-1, let the air region be replaced with sea water. Next, divide the region into an equal number of square areas so that an array of equally spaced points is obtained. Associate with each point P_o a voltage V_o and a conductance G_o. Associate voltages and conductances with the four points adjacent to P_o as indicated in Figure 4-2. Then Kirchoff's current law requires the sum of the currents into P_o to be zero; i.e.

$$I_1 + I_2 + I_3 + I_4 = 0 \tag{4-15}$$

$$(V_1-V_o)G_1+(V_2-V_o)G_2 + (V_3-V_o)G_3 + (V_4-V_o)G_4 = 0 \tag{4-16}$$

Solving Equation (4-16) for V_o yields

$$V_o = \frac{V_1G_1 + V_2G_2 + V_3G_3 + V_4G_4}{G_1 + G_2 + G_3 + G_4} . \tag{4-17}$$

The potential at any point may thus be found in terms of a weighted average of the potentials at adjacent points with the weights being functions of the conductivities associated with the points. For adjacent points having the same conductivity σ_{SW}, the conductance G connecting the two points is given by

$$G_{SW} = \frac{\sigma_{SW}\Delta Y}{\Delta Z} \text{ mhos/unit width in x} \tag{4-18}$$

where ΔY and ΔZ are the distance between points. For two adjacent points along the electrode having conductivity σ_e and cross-sectional height t in the y-direction, the conductance G_e is given by

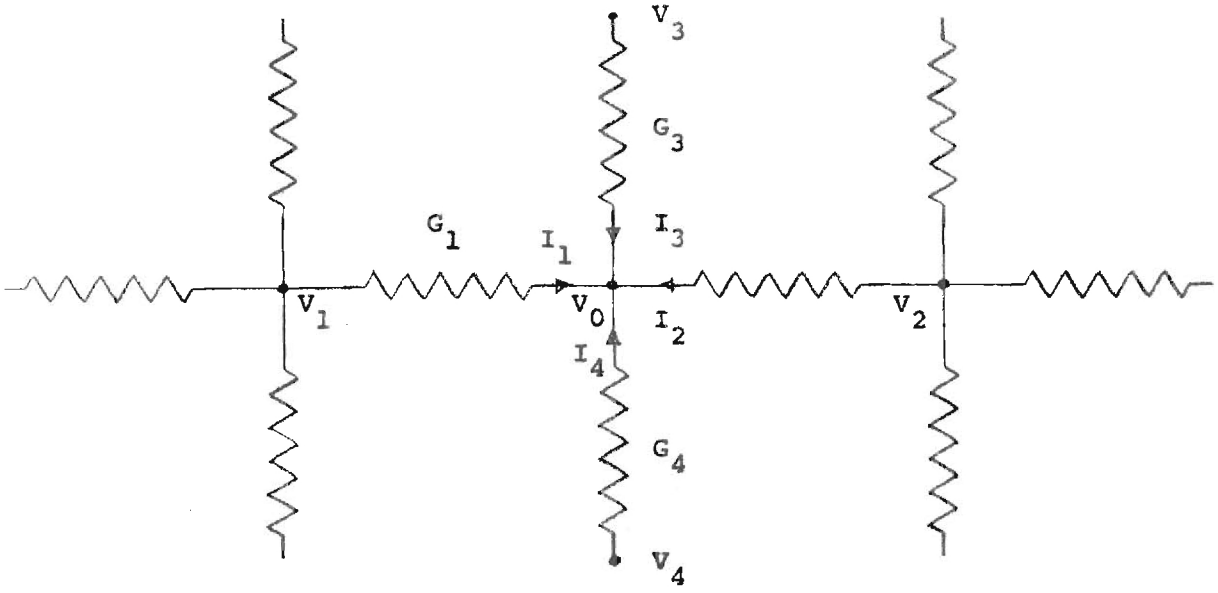

FIGURE 4-2. Circuit Representation of Kirchoff's Current Law

$$G_e = \frac{\sigma_e t}{\Delta Z} \text{ mhos/unit width in x} \qquad (4\text{-}19)$$

For two adjacent points where one point is on the electrode and the other point is in the sea water, the conductance G is given by Equation (4-18).

4.3 Computer-aided Solution of the Two-Dimensional Electrode Problem

The computer solution of the two-dimensional electrode problem starts with an initial estimate of the potential at each point in the array. Conductivities are assigned to each point to represent the material medium there. A series of contiguous horizontal points are used to represent each electrode. A driving potential $+V_s = +50V$ is assigned to one end point of one electrode (anode), and a driving potential of $-V_s = -50V$ is assigned to one end point of the other electrode (cathode). The driving potentials are not allowed to change during the course of the iterative computer procedure which seeks to find the values of potential at each point in the array such that Equation (4-17) is satisfied at each source-free point. At the points of driving potentials, the sum of the currents entering the positive ($+V_s$) terminal should equal the sum of the currents leaving the negative ($-V_s$) terminal. Moreover, the resistance between the terminals is given by

$$R = \frac{2V_s}{I} \text{ ohms/unit width in x} \qquad (4\text{-}20)$$

where I is the net current entering the positive terminal.

Figure 4-3 is a plot of the potential distribution obtained for two 45-meter aluminum electrodes spaced 90 meters apart ($\sigma_e = 4 \times 10^7$ mhos/m, t = 3 cm, $\sigma_{SW} = 4.3$ mhos/m). The electrodes are located at the top of the figure. The left end of each electrode is the terminal end (+50V, -50V). The lines on the graph are equipotential lines with the values in volts shown. Current lines (not shown) would be everywhere perpendicular to the equipotential lines.

Figure 4-4 shows the computed results for current leaving the electrodes and flowing into the sea water. The currents have been normalized. It is noted that the current distribution obtained is consistent with experimental data in that, for both anode and cathode, the current density is greater at each end than in the middle of each electrode. This result, though preliminary, is very encouraging.

Additional work is required to refine the computer-aided solution. Provisions are needed to allow for solutions in the case of the air-water interface (electrodes floating on the surface of the sea). Provisions are also needed to allow the specification of a composite electrode having a buoyant core, annular aluminum conductors, and carbon-loaded plastic jacket. Parametric studies on this type of composite electrode will be important in determining the parameters of the final design and in determining current densities and temperatures produced under operating conditions. Additional work is also needed to bring together the results of this analysis and those described in the next chapter concerning magnetic field calculations.

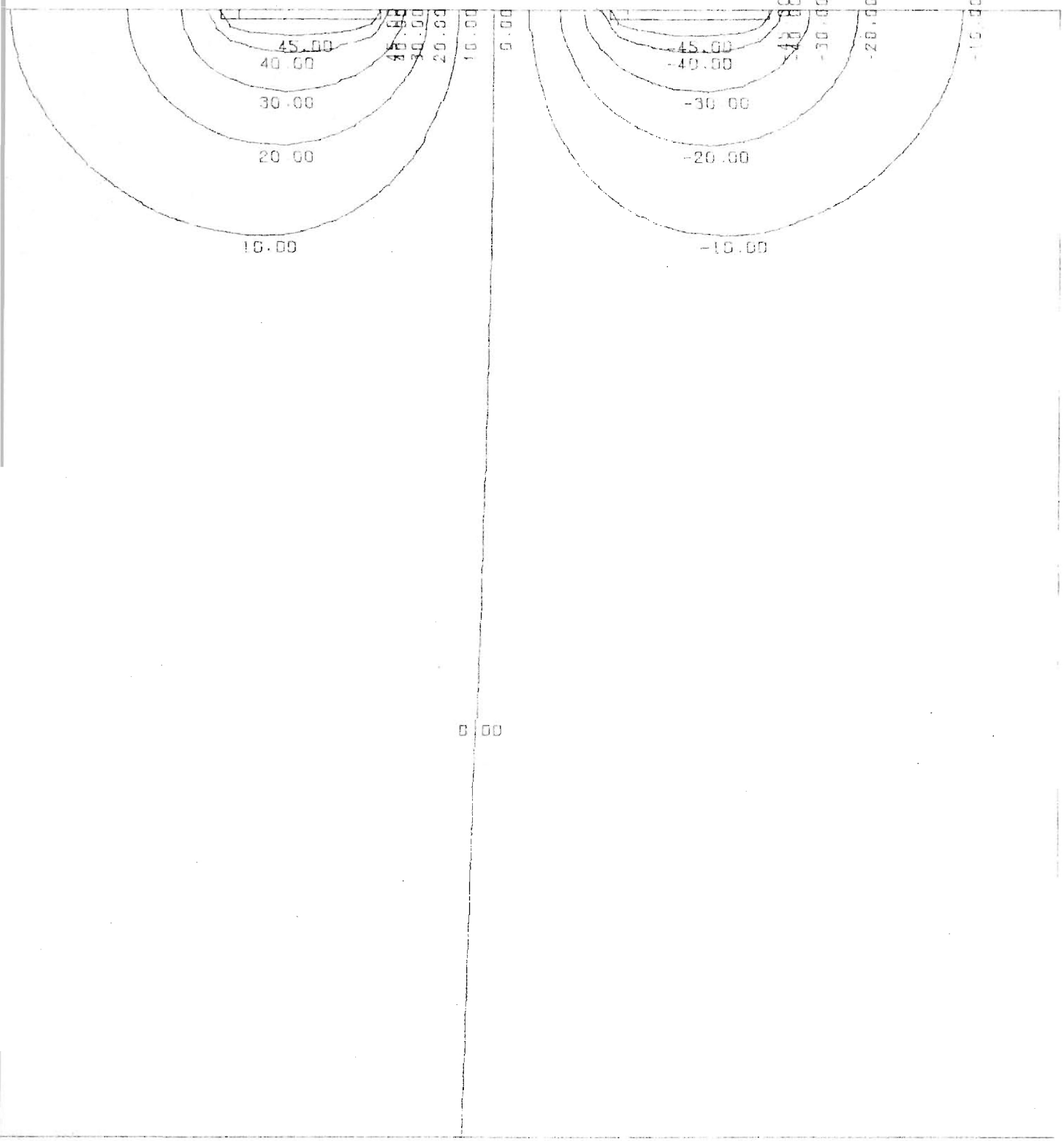

FIGURE 4-3. Calculated Potential Distribution for Two-Dimensional Electrode Geometry.

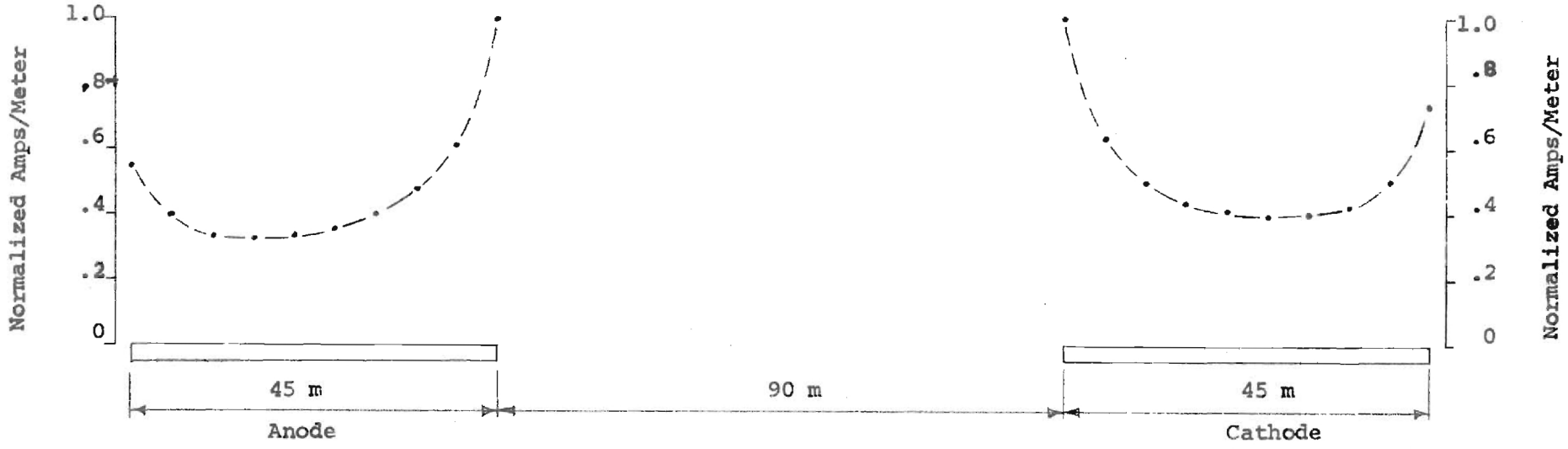

FIGURE 4-4. Calculated Current Distributions for Two-Dimensional Electrode Problem.

CHAPTER 5

CONSIDERATIONS FOR CALCULATING THE MAGNETIC FIELD

5.1 Introduction

The magnetic field produced by a current distribution in the sea has three sources. First, there is a component which is produced by the current flow in the water. Second, there is a component which is produced by the flow of current inside the electrodes submerged in the water. Third, there is a component which is produced by the current flow inside the connecting cable (S-cable) which connects the aft electrode to the voltage source. To calculate the total magnetic field for a given source voltage, it is necessary to know the total current which flows in the S-cable, the voltage distribution along the electrodes, and the voltage distribution in the sea water. The conductivity of the electrode material and of the sea water and these voltage distributions are sufficient to calculate the current distributions in the electrodes and in the water. From these current distributions, the respective magnetic field components can be calculated.

The numerical procedure for calculating the magnetic field first requires that the voltage distribution along the electrodes and in the water be calculated. This is a boundary value problem which can require an enormous computational facility unless symmetry can be exploited to reduce the problem from one which has a

three-dimensional geometry to one which has a two-dimensional geometry. It will be shown in the following section that this can be done with the geometry of the present problem. In the last section, a numerical procedure is presented by which the total magnetic field can be calculated. The most difficult aspect of this problem arises from the fact that the magnetic field at any point in the water depends on the current at every other point. Thus a numerical computation can be time consuming. This limitation has made it difficult to obtain any meaningful results at this time. However, it is felt that by optimizing the numerical procedures, the magnetic field computations can be made with reasonable computer run times.

5.2 Reduction of the Problem to a Two-Dimensional Geometry

Consider the two electrode systems illustrated in Figure 5.1. The electrodes lie on the surface of the sea water, and it is assumed that the sea depth is sufficiently large that the sea floor can be considered to lie at minus infinity. It is desired to show that the current distribution in the sea water is rotationally symmetric about the longitudinal axis of the electrode system. This will reduce the problem of solving for the current at all points in the sea to that of solving for the currents in only one plane, e.g., the y-z plane.

The time invariant Maxwell's equations for the system can be written

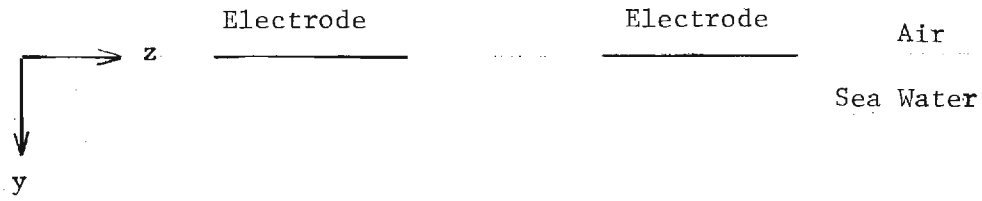

Figure 5-1. Illustration of two electrode system located in air to seawater interface.

$$\nabla \cdot \vec{E} = - \frac{\rho}{\epsilon} \tag{5.1}$$

$$\vec{J} = \sigma \vec{E} \tag{5.2}$$

$$\nabla \times \vec{H} = \vec{J} \tag{5.3}$$

$$\nabla \cdot \vec{J} = 0 \tag{5.4}$$

where $\vec{E}$ is the electric field intensity, $\vec{H}$ is the magnetic field intensity, $\vec{J}$ is the current density, ρ is the charge density, σ is the conductivity, and ϵ is the permittivity. Since there are two regions of space which have different σ and ϵ, it would follow that there are two solutions to these equations in general. However, it will be shown that, where the electrodes lie in the surface of the water, the electric field intensity is rotationally symmetric about the z-axis, i.e., the longitudinal axis of the electrode system. Thus a two region boundary value problem can be reduced to a single region one.

The solution to this problem requires that it be shown that the charge density ρ is zero at the interface between the water and the air, i.e., at $y = 0$. To do this, Equations (5.2) and (5.4) are first combined to yield

$$\begin{aligned} \nabla \cdot \vec{J} &= \sigma \nabla \cdot \vec{E} + \vec{E} \cdot \nabla\sigma \\ &= 0 \end{aligned} \tag{5.5}$$

Substitution of Equation (5.1) for $\nabla \cdot \vec{E}$ into this equation and solution for ρ yields

$$\rho = \frac{\epsilon}{\sigma} \vec{E} \cdot \nabla\sigma \tag{5.6}$$

In the present problem, σ is a function only of the y coordinate. Thus $\nabla\sigma$ can have only a y component. Since σ is constant for $y \neq 0$, $\nabla\sigma$ is zero except at $y = 0$. Thus a charge density ρ can only exist as a surface charge at the air to water interface at $y = 0$. However, by symmetry, the electric field intensity at $y = 0$ is parallel to this interface. Thus $\vec{E} \cdot \nabla\sigma = 0$ at $y = 0$ and the surface charge must be zero. This conclusion would not follow if the electrode system longitudinal axis did not lie in the air to water interface.

Since ρ is identically zero at all points for the assumed geometry, it follows that there are no boundary conditions to be imposed on the solution for the electric field intensity which are dependent on the constituitive parameters of the media. This follows from the boundary conditions at the air to water interface. These are

$$\hat{n} \cdot (\epsilon_2 \vec{E}_2 - \epsilon_1 \vec{E}_1) = \rho_s$$

$$= 0 \qquad (5.6)$$

$$\hat{n} \times (\vec{E}_2 - \vec{E}_1) = 0 \qquad (5.7)$$

where $\hat{n}$ is a unit vector normal to the interface, ρ_s is the surface charge density on the interface, and $\vec{E}_1$ and $\vec{E}_2$ are the electric field intensities on adjacent sides of the interface. Both Equations (5.6) and (5.7) are satisfied identically **and independently of the values of** ϵ_1 and ϵ_2 since the symmetry of the problem demands that $\vec{E}$ be tangential to the air to water interface. Thus all boundary conditions can be satisfied with only one electric field solution which can be written

$$\vec{E} = - \nabla\phi \tag{5.8}$$

where ϕ is a scalar function which from Equation (5.1) must satisfy

$$\nabla^2\phi = 0 \tag{5.9}$$

at all points external to the electrodes.

Symmetry demands that the solution for ϕ be constant on any circle which is perpendicular to and whose center coincides with the longitudinal axis of the electrodes. Thus, the solution for ϕ in the y - z plane is identical to the solution in any other plane which is generated by a rotation of the y - z plane about the z-axis of Figure 5.1. It follows then that the complete solution for ϕ can be obtained by solving only the two-dimensional Laplace equation **in cylindrical coordinates**

$$\frac{\partial^2\phi}{\partial r^2} + \frac{\partial^2\phi}{\partial z^2} + \frac{1}{r}\frac{\partial\phi}{\partial r} = 0 \tag{5.10}$$

subject to the boundary conditions on the electrode surfaces and at infinity. Once the potential distribution in the water is obtained by solution of this equation, the current density in the water follows from Equations (5.2) and (5.8) which yield

$$\vec{J} = - \sigma \nabla\phi \tag{5.11}$$

A numerical solution for determining the magnetic field generated by this current distribution is presented in the following section.

5.3 Magnetic Field Computation

The method of calculating the magnetic field which is developed in this section is based on the application of the law of Biot-Savart. With reference to Figure (5.2), this law states that the magnetic flux density $\Delta\vec{B}$ generated by a current I flowing along a vector distance $\Delta\vec{r}$ is given by

$$\Delta\vec{B} = \frac{\mu_o I}{4\pi} \frac{\Delta\vec{\ell} \times \hat{r}_{QP}}{r_{QP}^2} \tag{5.12}$$

where μ_o is the free-space permeability, r_{QP} is the distance from point Q to point P, and $\hat{r}_{QP}$ is a unit vector which points from Q to P.

Consider the geometry of Figure (5.3). The magnetic field at point P is to be calculated from a known potential distribution on the two electrodes and in the water and from a known current in S-cable. An application of Equation (5.12) to the connecting electrode yields

$$\vec{B} = - \hat{x} \frac{\mu_o I}{4\pi y_o} (\sin\alpha - \sin\beta) \tag{5.13}$$

where $\hat{x}$ is a unit vector in the x-direction.

The component of the magnetic field at P from the current flowing in the electrodes can be determined by summing the contributions from the electrode elements between the points at which the potential is known. If ΔR_E is the electrode resistance between these points, the field at P due to the current flowing between the ith and ith + 1 points is given by

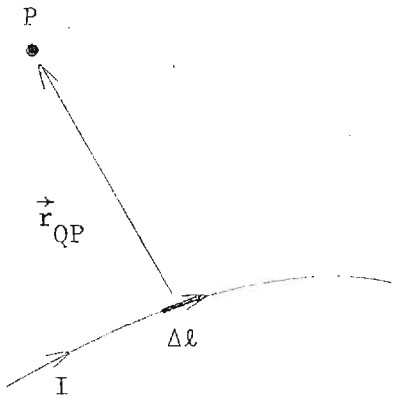

Figure 5.2 Illustration for application of Biot-Savart Law.

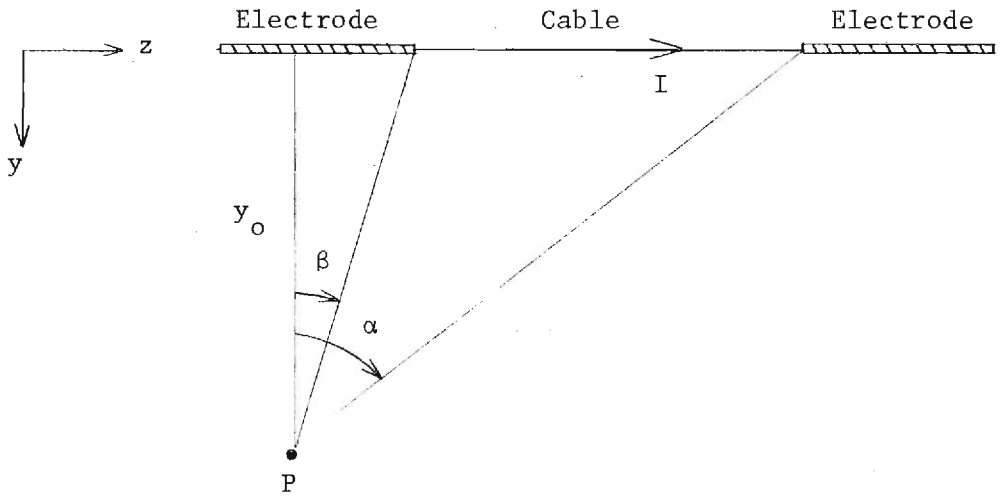

Figure 5.3 Illustration for the calculation of magnetic field set up by current in the connecting cable between electrodes.

$$\Delta\vec{B} = - \hat{x} \frac{\mu_o}{4\pi y_o} \frac{\phi_{i+1} - \phi_i}{\Delta R_E} (\sin\theta_i - \sin\theta_{i+1}) \qquad (5.14)$$

The total magnetic field generated by the current in the electrodes can be obtained by summing the $\Delta\vec{B}$ contributions over the length of both electrodes.

The exact magnetic field component at P produced by the current in the water requires an integration of Equation (5.12) over the current density $\vec{J}$ in the water. For the present problem, this is not possible since $\vec{J}$ is not known at every point. Only the electric potential distribution at a finite set of points is assumed to be known. Thus an approximation is required which will make a numerical solution possible. To obtain this, consider the curvilinear volume element illustrated in Figure 5.4. It is assumed that the longitudinal axis of the electrodes coincides with the z-axis so that the potential is constant with polar angle ω. Thus it follows from Equations (5.2) and (5.8) that there is no φ component of current in the volume element. The approximation involves replacing the current density in the volume by two perpendicular current elements I_r and I_z which flow through the center of the volume element. To obtain these, it will be assumed that the electric potential varies linearly between adjacent points at which it is assumed to be known. With this assumption, the potential inside the volume element can be written

$$\phi = \phi_{ij} + (\phi_{i,j+1} - \phi_{i,j}) \frac{z-z_i}{z_{i+1}-z_i} + \left[\phi_{i+1,j} - \phi_{i,j} + (\phi_{i+1,j+1} - \phi_{i+1,j} - \phi_{i,j+1} + \phi_{i,j}) \frac{z-z_i}{z_{i+1}-z_i}\right] \times \frac{r-r_i}{r_{i+1}-r_i} \qquad (5.15)$$

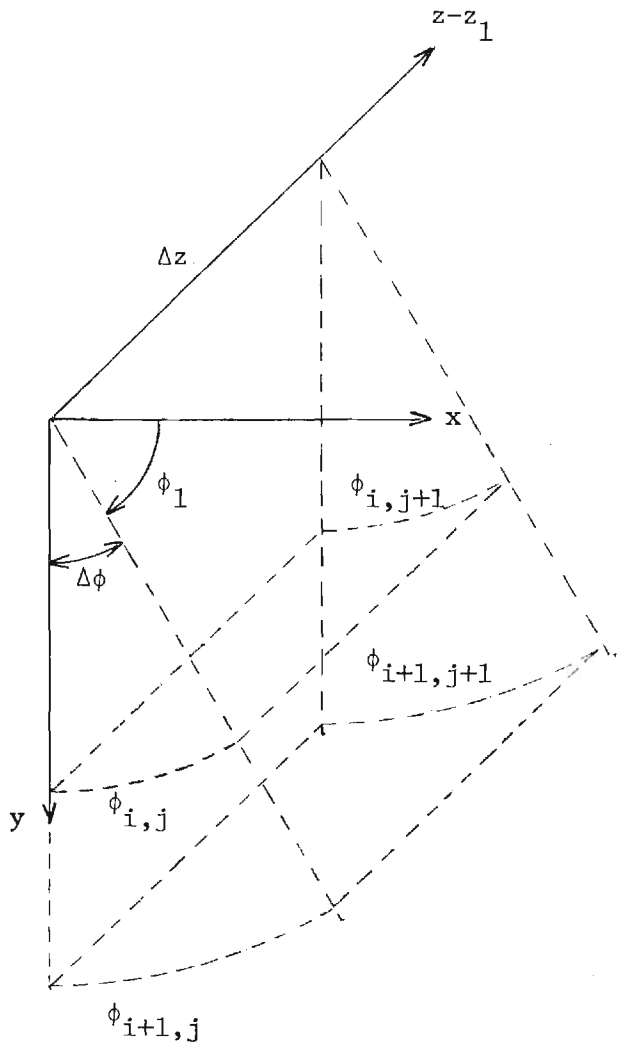

Figure 5.4. Illustration of volume element for calculation of magnetic field set up by current in the water.

where $z_i \leq z \leq z_{i+1}$ and $r_i \leq r \leq r_{i+1}$. In the following it will be assumed that $z_{i+1} - z_i = r_{i+1} - r_i = d$.

The solution for the total current flowing in the r and z directions in the volume element is obtained from (5.15) as follows:

$$I_r = \int_0^{\Delta\varphi} \int_0^{\Delta z} \sigma\left(-\frac{\partial\phi}{\partial r}\right) r \, d\varphi' \, dz' \tag{5.16}$$

$$I_z = \int_0^{\Delta\varphi} \int_0^{\Delta z} \sigma\left(-\frac{\partial\phi}{\partial z}\right) r \, d\varphi' \, dr' \tag{5.17}$$

where $\varphi' = \varphi - \varphi_i$, $r' = r - r_i$ and $z' = z - z_i$. A solution for I_z yields

$$I_z = \frac{\sigma \Delta\varphi}{2} \left[(\phi_{i,j} - \phi_{i,j+1})(r_i + \frac{d}{3}) + (\phi_{i+1,j} - \phi_{i+1,j+1})(r_i + \frac{2d}{3}) \right] \tag{5.18}$$

A solution for I_r yields an expression which is a function of r. It can be shown that setting $r = r_i + \frac{d}{2}$ in this expression is equivalent to averaging I_r over the volume element. This yields the expression

$$I_r = \frac{\sigma \Delta\varphi}{2} (r_i + \frac{d}{2}) \left[(\phi_{i,j} - \phi_{i+1,j}) + (\phi_{i,j+1} - \phi_{i+1,j+1}) \right] \tag{5.19}$$

To obtain the magnetic field associated with these current elements, the contributions of each one must be summed. It will be assumed that each current element lies in the center of its respective volume element. Let the observation point P have the position vector

$$\vec{r}_P = \hat{r}(\ell - 1)d + \hat{z}(m - 1)d \tag{5.20}$$

where ℓ, m, and n are positive integers. The position vector of any one current element can be written

$$\vec{r}_Q = \hat{r}'(i - \tfrac{1}{2})d + \hat{z}(j - \tfrac{1}{2})d \tag{5.21}$$

where

$$\hat{r} = \hat{x}\cos\varphi + \hat{y}\sin\varphi \tag{5.22}$$

$$\hat{r}' = \hat{x}\cos\varphi + \hat{y}\sin\varphi' \tag{5.23}$$

and

$$\varphi = (n - 1)\Delta\varphi \tag{5.24}$$

$$\varphi' = (k - \tfrac{1}{2})\Delta\varphi \tag{5.25}$$

where $\Delta\varphi$ is the azimuthal angle subtended by each volume element. The vector distance between points P and Q is then

$$\vec{r}_{QP} = \hat{x}\, d[(\ell - 1)\cos\varphi - (i - \tfrac{1}{2})\cos\varphi'] + \hat{y}\, d[(\ell - 1)\sin\varphi - (i - \tfrac{1}{2})\sin\varphi'] + \hat{z}\, d[m - j - \tfrac{1}{2}] \tag{5.26}$$

The preceding expressions can be used in Equation (5.12) to calculate the vector contribution of the magnetic field at P from the r and z current elements located at Q as follows:

$$\Delta\vec{B} = \frac{\mu_o}{4\pi} \frac{d(\hat{r}I_r + \hat{z}I_z)x\vec{r}_{QP}}{r_{QP}^3} \tag{5.27}$$

This equation results in three orthogonal components for $\Delta\vec{B}$ given by

$$B_x = \frac{\mu_o}{4\pi} \frac{d^2}{r_{QP}^3} \left[I_r \sin\varphi'(m - j - \tfrac{1}{2}) - I_z[(\ell - 1)\sin\omega - (i - \tfrac{1}{2})\sin\varphi'] \right] \quad (5.28)$$

$$B_y = \frac{\mu_o}{4\pi} \frac{d^2}{r_{QP}^3} \left[- I_r \cos\varphi'(m - j - \tfrac{1}{2}) + I_z[(\ell - 1)\cos\omega - (i - \tfrac{1}{2})\cos\varphi'] \right] \quad (5.29)$$

$$B_z = \frac{\mu_o}{4\pi} \frac{d^2}{r_{QP}^3} \left[I_r \cos\varphi[(\ell - 1)\sin\omega - (i - \tfrac{1}{2})\sin\varphi'] - I_r \sin\varphi'[(\ell - 1)\cos\varphi - (i - \tfrac{1}{2})\cos\omega'] \right] \quad (5.30)$$

These equations have been programmed on the CDC Cyber 74 computer at Georgia Tech. However, due to the extremely long computation times required to obtain the magnetic field at an array of points, no meaningful results can be reported on the electrode problem as this time. However, it is felt that the computations can be optimized to significantly reduce the computation times. As an example of the computational complexity of this problem, suppose that the potential ϕ is known at an array of points in the y-z plane of size 65×65. Suppose it is desired to calculate the magnetic field at a 65×65 array of points in the azimuthal plane defined by $\omega = 90°$. Also, suppose the azithmul angle subtended by each curvilinear volume element is taken to be 22.5°. The magnetic field calculations could be set up on the computer as a sequence of nested "loops", with a total number of loop calculations given by $65 \times 65 \times 8 \times 64 \times 64 = 138,444,800$.

CHAPTER 6

PROPOSED CARBON POLYMER JACKETED ELECTRODE

Within the last five years, the power industry has been experimenting with conductive jackets for underground power distribution cables. Their goal is the prevention of corrosion to the outer copper or aluminum cable conductors which are normally in direct contact with the earth. As this report is being prepared, final tests of these new conducting jacketed power distribution cables are taking place at the McGraw Edison High Voltage Research Laboratory in Franksville, Wisconsin, under the sponsorship of the Electric Power Research Institute. Georgia Tech is participating in the analysis and prediction of these test results. Many of the same types of computations involving voltage distributions and current densities are involved in the minesweeping electrode problem. Knowledge of the properties and test results of these new cable materials has led to the proposed application of these materials to the high-current minesweeping electrode.

The proposed electrode has a configuration shown in Figure 6-1. This electrode configuration is similar to present electrodes except at the outer periphery. The round aluminum strands normally used in aluminum electrodes are replaced with flat aluminum conductors to increase surface smoothness and decrease outer radius while retaining cable flexibility. The amount of aluminum can be reduced by almost

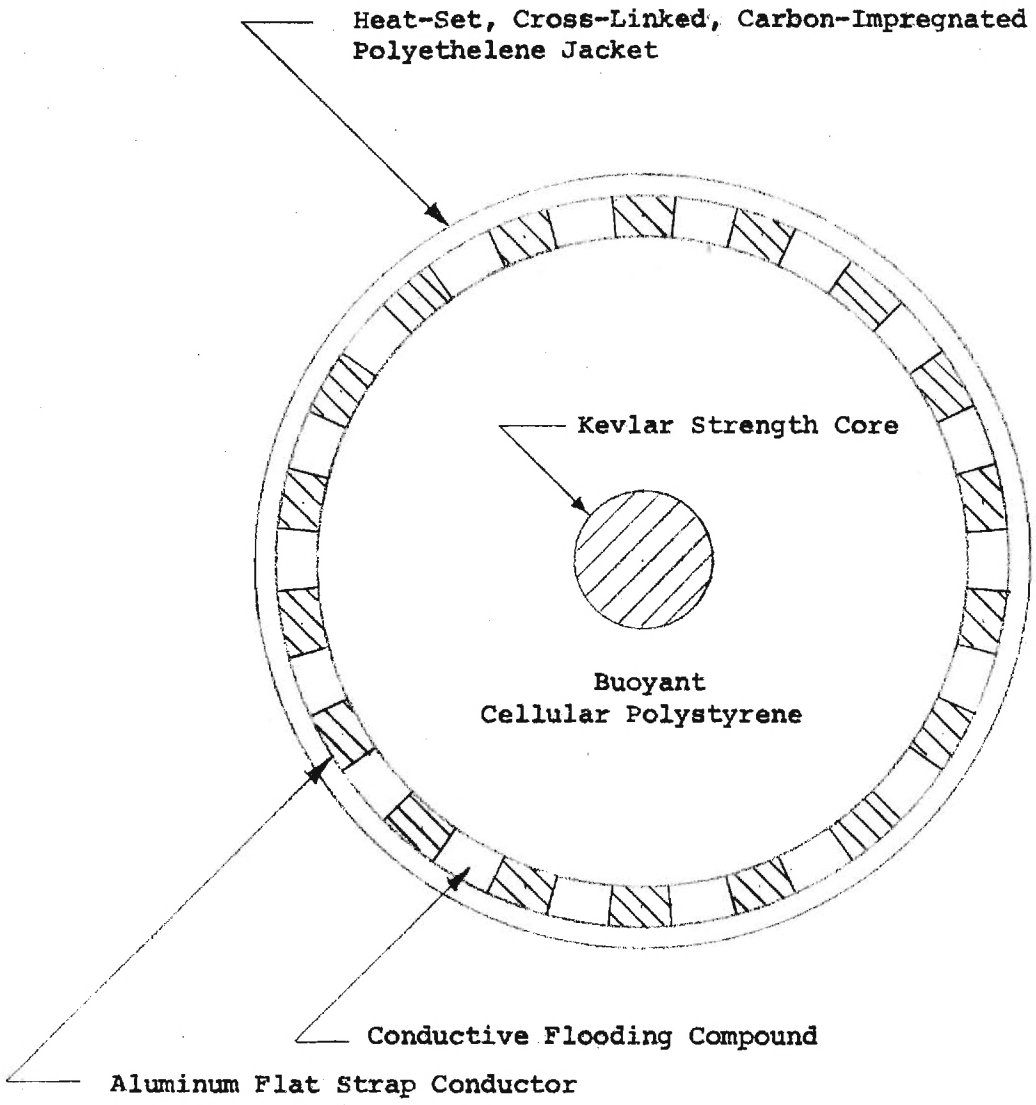

FIGURE 6-1. Construction Details for Jacketed Electrode.

a factor of 2 since no additional aluminum is needed for dissolution into the sea. The effect of decreasing the amount of aluminum in the electrode is an increased resistance; however, as previously demonstrated, this has small impact on total system resistance.

The aluminum conductors are jacketed in heat-set, cross-linked, carbon-impregnated, polyethelene material. This jacket serves many purposes. First, it shields the aluminum conductors from the corrosive action of the sea water. Second, it conducts electrode current from the aluminum conductors to the sea water. Third, it conducts the electrode heat generated by resistive heating in the aluminum conductors from the aluminum to the sea water. Fourth, it decreases drag by providing a smooth surface in contact with the sea water instead of the rough, spiral aluminum conductors which may be fouled at the aft ends due to birdcaging. And fifth, it makes the electrode easier to handle and stow.

The spaces between the aluminum straps and the conducting jacket are filled with a conducting flooding compound which likewise serves many purposes. First, it prevents the spreading of sea water throughout the electrode should a hole develop in the conducting jacket. Second, it lowers the resistance of the electrode by lowering the "radial" resistance from the aluminum strap to the sea. And third it helps conduct heat from the aluminum to the sea water in the same manner as it conducts current to the sea water.

Figure 6-1 also shows a central Kevlar strength core. This core is not necessarily needed for the jacketed cable since the aluminum conductors can now be used as the strength member of the electrode. By eliminating the Kevlar core, a slight decrease in the diameter of

the electrode due to the greater buoyancy of a purely polystyrene core is afforded.

Two preliminary electrode designs have been prepared, one for replacement for the PE-3 electrode and one with a larger ampere capacity (ampacity). Tables 6-1 and 6-2 show key parameters of these electrode designs. Table 6-1 compares PE-3 parameter values with the parameters of the proposed replacement (herein referred to as the PE-X). Table 6-2 gives preliminary specifications for the proposed PE-X electrode.

As shown in Table 6-1 the proposed electrode and the PE-3 are very similar. The significant differences are that the amount of aluminum in the proposed electrode has been reduced and substituted with conducting jacket. This is noticable in the increased resistance of the electrode (an increase of 27%); however, this increases the total system resistance by only 2.7%. Another noticable difference is the increased lifetime of the proposed electrode which is estimated to be 10 years. Obviously there is no way to estimate the life of the proposed electrode. This electrode, however, in many respects resembles the construction of S-cable, many of which last 10 years in normal operation. The life of the proposed electrode may be limited by handling considerations. There is probably a limit as to how many punctures the proposed electrode could sustain before the underlying aluminum would be severed due to sea water anodic erosion. It must be emphasized that the conducting jackets proposed are very flexible and and pliable and meet very stringent power industry standards for handling under severe weather conditions. The cables must also withstand being reeled and stowed on small diameter spools.

TABLE 6-1. Comparison of Proposed and PE-3 Electrodes

PARAMETER	PROPOSED	PE-3
LENGTH:	150 FT.	150 FT.
DIAMETER:	3.41 IN.	3.41 IN.
HEAD OF TAIL SEPARATION OF ELECTRODES:	300 FT.	300 FT.
BUOYANCY:	.97	.97
SUBMERGENCE:	NONE	NONE
ELECTRODE RESISTANCE:	.00206 OHMS	.00162 OHMS
SEAWATER RESISTANCE:	.0212 OHMS	.0212 OHMS
SURFACE ROUGHNESS (λ):	.001	.005
DRAG AT 30 KNOTS AT SURFACE:	1245 POUNDS	1680 POUNDS
LIFETIME:	10 YEARS ?	< 20 HOURS
COST:	SAME AS PE-3	?
HANDLING:	BETTER THAN PE-3	GOOD
STOWAGE CORROSION:	NONE	FAIR
EXPLOSION PROTECTION:	SAME AS "S" CODE	GOOD
ATTACHMENT:	SAME AS PE-3	GOOD
WEIGHT:	525 POUNDS	525 POUNDS

TABLE 6-2

Proposed Electrode (Preliminary)

Length:	150 ft.
Diameter:	3.5 inches
Head to Tail Separation:	300 ft.
Bouyancy:	.94 - .97
Submergence:	10 ft.
Electrical Resistance:	
1. Sea Path:	.0112 ohms
2. S Cable:	.006 - .008 ohms
3. Electrode:	.003 ohms
Surface Roughness:	.001λ
Drag at 30 Knots:	1250 Pounds (Total)
Lifetime:	10 years (?)
Cost:	Same as PE-3
Handling:	Better than PE-3
Stowage:	Coiled on 6 foot diameter reel
Stowage Corrosion:	None
Strength Member:	Aluminum Conductors
Cross-sectional Area of Aluminum:	2250 MCM
Jacket Thickness:	0.1 inch

The proposed PE-X electrode specified in Table 6-2 has many of the same characteristics of the proposed PE-3 electrode. Noticable differences are a slightly greater diameter and a specification for submergence to a depth of 10 feet for normal operation. The primary reason for the 10-foot submergence is the lower sea path resistance and greater cooling capacity required. Both proposed jacketed electrodes are expected to produce less drag than corresponding bare aluminum electrodes due to the increased smoothness of the outer surface of the electrode. This increased smoothness is predicted to result in 24% less electrode drag. Table 6-3 summarizes the advantages and disadvantages of the carbon polymer electrode design concept.

Key specifications for carbon polymer jacket material are electrical resistivity and thermal resistivity. The greater the carbon loading of the base polyethelene material the lower both of these resistances. Too great a carbon loading results in a brittle, non-pliable material. The power industry is nearing a decision as to the exact amount of loading. The amount predicted is near 40% loading. This percentage has little impact on the handling characteristics of unloaded polyethelene and yet is high enough to give good thermal and electrical resistance properties.

The electrical circuit of a minesweeping electrode system using a conducting jacketed electrode has two additional series resistors in the circuit due to the two electrode jackets. The equation for these additional resistances for an electrode of length L and diameter D with a jacket of thickness T is given by

$$R_{jacket} = \frac{\rho T}{\pi D L} \qquad (6\text{-}1)$$

TABLE 6-3

Benefits of Carbon Filled Polymer Jacketed Aluminum Electrodes

1.	Lifetime:	Orders of magnitude greater than bare aluminum
2.	Cost:	Approximately the same initial cost, cost per hour less than 1% of present cost
3.	Drag:	Approximately 25% less due to increased smoothness
4.	Handleing:	No birdcaging of electrodes

DISADVANTAGES

1. Increase of 2.7% in total circuit resistance
2. No in house remanufacture of electrodes

where ρ is the electrical resistivity of the jacket material. Preliminary estimates from power industry measurements and cable manufacturers' specifications show that resistivity ρ in the range from 50 to 100 ohm-cm can be expected. (The thermal resistivity ρ_T is expected to be approximately 350°C-cm/watt.)

CHAPTER 7

NOBLE METAL ELECTRODES

7.1 Introduction

Platinum is the most widely used noble metal electrode material, and one of the best electrode materials known. It exhibits high exchange current density (low overvoltage) for many redox reactions, and its dissolution rate is very low in most environments. However, the use of platimum for electrodes has been limited to laboratory applications because of the high cost of the metal.

In recent years platinized electrodes have been developed for the industrial use in cathodic protection against corrosion. They combine the effectiveness of platinum with a reasonable cost and other desirable properties of the base materials. At first, attempts were made to use as base materials relatively noble metals such as silver or copper.[1,2] The electrodes were not very practical nor successful because any uncoated area suffered heavy deterioration. The solution of this problem was found in the use of "valve" metals, such as titanium, niobium (columbium) and tantalum. These metals form on the surface a very stable oxide film with high electrical resistance, which protects the metal against corrosion even at high potentials used in cathodic protection. The film is "self-healing", i.e., a new film forms quickly when the surface is mechanically disturbed.

---

[1] I. D. Gessow, "Navy Experimental Work with Cathodic Protection," Corrosion, 12, 100 (1956).

[2] E. E. Nelson, "An Impressed Current Cathodic Protection System Applied to a Submarine," Corrosion, 13, 122 (1957).

In the presence of chlorides in the environment the protective film can break down locally, and a rapid localized corrosion (pitting) takes place. The breakdown occurs only above a certain characteristic critical potential (breakdown potential, pitting potential), which must not be exceeded in the use of the electrode. In the group of titanium, niobium and tantalum, titanium has the lowest breakdown potential, and tantalum the highest.

Standard commercial platinized electrodes are usually in the form of wires or rods. To improve the conductivity, copper-core electrodes are sometimes used. The important properties of various electrode materials are summarized in Table 7-1.

Platinized electrodes have been used mainly for active cathodic protection of steel structures in sea water, such as offshore platforms[3] and navy ships[4,5]. In this application the electrodes are always used as anodes.

Table 7-1

Properties of the Anode Base Materials

Metal	Breakdown Potential (V)	Resistivity microohm-cm	Annealed Tensile Strength (psi)
Titanium	8 to 14	48 to 70	50,000 to 100,000
Columbium	70	13.2	45,000 to 60,000
Tantalum	180	12.4	60,000 to 80,000

[3] G. L. Doremus and J. G. Davis, "Marine Anodes: Old and New," Materials Protection, 6, 30 (1967 - January).

[4] H. S. Preiser and F. E. Cook, "Cathodic Protection of an Active Ship Using a Trailing Platinum-Clad Anode," Corrosion, 13, 125 (1957).

[5] H. S. Preiser and B. H. Tytell, "Some Platimum Anode Designs for Cathodic Protection of Active Ships," Corrosion, 15, 596 (1959).

7.2 Performance of Platinized Electrodes as Anodes in Sea Water

When a positive current passes through an inert electrode into an electrolyte containing chlorides, such as sea water, the principal anodic reactions involve evolution of oxygen and chlorine, according to reactions

$$2\ H_2O = O_2 + 4\ H^+ + 4\ e^- \qquad (7\text{-}1)$$

$$2\ Cl^- = Cl_2 + 2\ e^- \qquad (7\text{-}2)$$

Although reaction (7-1) is thermodynamically preferred (lower equilibrium potential), the kinetic factors make reaction (7-2) dominant.

A platinum (or platinized) electrode is not completely inert. At sufficiently high noble potentials it passivates and covers with a protective oxide film. It was found that the dissolution rate of platinum can be excessive when the current density is below the critical current density for passivation i_p, but negligible above i_p.[6] In 1M NaCl (5.9 weight %) the crictical current density was found to be $i_p = 6.4 \times 10^{-3}$ A/cm^2 (0.0413 A/in^2) at the potential of +1.43 V.[6]

The consumption of platinum from the platinized electrodes in sea water usually ranges from 0.2 to 1.0 μg/A-hr.[7] Commercial platinized columbium wire electrodes with a standard 100 μin coating of platinum are rated at about 500 A-years/ft^2 (0.53 A-years/cm^2), which corresponds to a dissolution rate of about 1.2 μg/A-hr. The dissolution rate per A-hr is almost independent of the current density used (above the

---

[6] J. A. Bittles and E. L. Littauer, "Anodic Corrosion and Passivation of Pt in Cl$^-$ Solution," Corr. Sci., 10, 29 (1970).

[7] M. A. Warne and P. C. S. Hayfield, "Platinized Titanium Anodes for Use in Cathodic Protection," Materials Performance, 15, 39 (1976 - March).

critical current density for passivation)[7]. Platinized titanium anodes are usually used at current densities of about 100 A/ft^2 (0.7 A/in^2), although higher current densities (up to 500 A/ft^2, 3.5 A/in^2) can be used without an increase in the dissolution rate per A-hr. Platinized niobium and tantalum can be used at current densities up to 1000 A/ft^2 (7 A/in^2) and probably even higher.

The breakdown potential of the substrate materials depends on the metal (see Table 7-1) and the chemistry of the environment, especially the concentration of halides. As chloride concentration increases, the breakdown potential decreases. On the other hand, the potential of the electrode for a given anodic current density will be lower at higher chloride concentrations. The exact limiting conditions have to be determined experimentally. The potential of the electrode is the potential difference between the metal and the electrolyte across the boundary double layer; it depends on the current density and the polarization characteristics in the given electrolyte. The total voltage as measured at the source is thus the sum of the two electrode potentials and the IR drop in the electrolyte.

7.3 Performance of Platinized Electrodes as Cathodes in Sea Water

A platinum electrode is a very effective cathode in water because of the high exchange current density for the main cathodic reaction,

$$2\ H^+ + 2\ e^- = H_2 \qquad (7\text{-}3)$$

For platinized electrodes, the effect of large amounts of atomic hydrogen available at the metal surface must be considered. The atomic hydrogen absorbs in the surface and can diffuse in the metal; if the material is susceptible to hydrogen embrittlement, a serious deterioration of mechanical properties can result. Tantalum and niobium are highly susceptible to hydrogen embrittlement; titanium is also susceptible, but to a lesser degree. However, since anodic dissolution and breakdown of passivity is not a problem on the cathode, other substrate materials may be selected. The main requirements would be the resistance to hydrogen embrittlement, good corrosion resistance in the presence of platinum, low cost, etc.

No data are available on the possible fouling of platinized cathodes by deposition of compounds from sea water; this aspect will have to be examined experimentally.

7.4 Cost of Platinized Electrodes

The most economical way to use platinized electrodes is to use standard products and operate the electrodes at relatively high current density. For example, the cost of a standard niobium wire with 100 μin layer of platinum can be as low as $0.34/A. If operated at 1,000 A/ft^2 (7 A/in^2), the estimated life is then 6 months. When lower current densities are used the life and cost increase proportionately.

For an electrode made from non-standard parts, such as custom-platinized niobium or tantalum strips, only a rough cost estimate can be made at this time. Based on the cost of the material, platinizing, and the cost of other parts and assembly, this rough estimate indicates a cost of about $15,000 to $20,000 for a high-current electrode.

CHAPTER 8

CONCLUSIONS AND RECOMMENDATIONS

8.1 Conclusions

8.1.1 Electrical Analyses and Jacketed Electrodes

A number of conclusions may be drawn from the results of the electrical analysis of the open loop minesweeping electrode system presented in Chapters 2 and 6:

(1) Minimum circuit resistance is desired to minimize generator power requirements;

(2) The sea water path resistance is the dominant and controlling term in the total circuit resistance and can be reduced by increasing electrode surface area, decreasing electrode separation, and/or increasing electrode submergence;

(3) Hydrodynamic drag increases with electrode surface area at a rate greater than linearly such that any decrease in generator power requirements due to reduced circuit resistance would be more than offset by an increase in towing power requirements;

(4) The sea water path resistance dictates that for existing and planned power generation and towing capacities, the surface area and geometry of the electrode system is basically fixed, regardless of electrode composition;

(5) The conductive jacket electrode in Figure 6-1 offers a very promising approach to the realization of a high-current, long-life minesweeping electrode.

From Chapters 4 and 5, it is concluded that analyses to determine current distributions on the electrodes more accurately are feasible. Calculations of the magnetic field produced from a given current distribution present some formidable obstacles in computation requirements; however, it is felt that rotational symmetries may be exploited to produce practical results in reasonable times. Accurate models of the electrical behavior of the open loop minesweeping electrode system will be very important in the final design of new electrodes.

8.1.2 Aluminum Electrodes

The indepth evaluation of the electrochemical properties of aluminum both as an anode and cathode material was presented in Chapter 3. Aluminum, due to the fact that it enters the electrolyte in a +3 valence state, would be the best dissolvable metal to use as an anode material. It is obvious from the analysis of this data that aluminum can provide only limited life in higher power applications, particularly with increased current density. The .83 amp current density was calculated from the maximum dissolution of PE3 electrodes. This provides a fairly effective way of measuring the maximum current density in the area of most rapid deterioration of the electrode. It is obvious that for 3.5 - inch diameter, 150-foot electrodes, any increase in current density beyond this value would result in rapid deterioration and life expectancies far less than presently obtained.

Even increasing the total amount of aluminum by increasing the diameter of the electrode and lengthening the electrode (to reduce total current density) provides only limited relief. This is obvious from tests that have already been conducted by the Navy on 300-foot, 4.5 - inch diameter bouyant aluminum electrodes. Therefore, it is obvious, not only from the economics of the project, but on availability of material, drag, inventory, etc., aluminum can only be considered a last resort as an alternative to some type of noble conductor as anode in the higher power system.

Analysis of cathodic deposits and cathodic corrosion of aluminum cathodes show that a life expectancy of aluminum electrodes serving this function would be a maximum of 180 hours. This, of course, would require a short end of sweep anodic pulse to remove cathodic deposits and provide a useful conductive surface for the next sweep. This short pulse would produce anodic corrosion and has been considered in the overall calculation. To verify the possibilities of aluminum cathodes, one must analyze the efficiency of the removal of cathode products by the anodic pulse at the end of each sweep, and the anodic and cathodic deterioration must be measured under expected conditions to be able to anticipate a true cathodic life for aluminum. If present predictions prove reliable, then the use of aluminum as a cathodic material for limited life is a possibility and the economics of an effective trade-off would have to be established versus noble cathodic conductors.

8.1.3 Platinized Electrodes

Platinized anodes are a relatively recent, but already proven

technology, which provides very efficient and long-lasting electrodes. Large current capacity can be achieved at a relatively low cost. If other considerations dictate a very long electrode, platinized wires or strips can be wrapped around a buoyant cable and attached at intervals to the current carrying wire core of the cable. A preliminary analysis has shown that if standard commercial products are used, the total required electrode can be made of a number of about fifteen feet long segments, each carrying into the water a current of 500 A (10 segments for a 150 foot long, 5,000 A electrode, 20 segments for a 300 foot long, 10,000 A electrode). The segments would be interconnected via sleeves attached to the wire core of the cable. For the anodes, the most suitable base materials are columbium and tantalum, which exhibit a high resistance to breakdown in sea water. The proposed electrode, although more expensive than the most efficient small size electrode, nevertheless would not be exceedingly expensive.

Same basic design can be used for the negative electrode (cathode). However, in view of the susceptibility of the most common anode materials to hydrogen embrittlement, other platinizable materials with desired properties, such as copper, copper-nickel alloys, stainless steel, etc., should be examined and tested.

Sufficient data on the performance of platinized electrodes in sea water are available in the literature for the application in cathodic protection. However, since the electrodes are normally not subjected to the high speeds involved in the minesweeping operations, it will be necessary to test the electrodes under those conditions

for durability and performance characteristics. The tests should include measurements of the polarization behavior in sea water at various flow rates up to 30 knots, long-term tests of the performance at high flow rates, and mechanical tests of the electrode materials following periods of use.

Somewhat more detailed tests will be required for the cathodes, to determined, in addition to the electrode performance, the susceptibility to hydrogen embrittlement. Several platinized base materials may have to be tested before the final selection is made.

8.2 Recommendations

It is recommended that a program of development be undertaken to develop both conductive jacket electrodes and platinized electrodes for high-current, open loop minesweeping systems.

The recommended effort would begin with scale-model laboratory testing of the proposed electrode configurations and the further development of the analytical tools which will eventually be required for full-scale design. Based on the data obtained from the laboratory tests and theoretical studies, a full-scale electrode system would be designed for ultimate implementation and sea trials by the Navy.

APPENDIX A

CALCULATION OF SPECIFIC GRAVITIES IN SUB-BUOYANT STRUCTURES

The angle, ϕ_c, that a towed cable with a free end makes with the horizontal is governed by the equation:

$$W = R\sin\phi_c \tan\phi_c$$

where W is the weight in water per unit length of cable and R is the drag per unit length of cable when the cable is normal to the stream. When the length of cable (here assumed to be 150 feet) and the depth of submergence are specified, ϕ_c is determined. R is equal to $\frac{1}{2}C_n\rho_{H_2O}V_n^2 D_o$ where D_o = cable diameter, V_n = towing speed, ρ_{H_2O} = density of water, and C_n is the drag coefficient which is available in tabulated form as a function of Reynold's number (which depends on the towing speed and cable geometry). Since we are considering a cable whose geometry is known, R is specified when the speed is given (which for purposes of calculation was chosen to be 5 knots and 15 knots), and thus W can be determined from the equation given above. From W, SG for Configuration 1 and SG_{core} for Configuration 2 of Figure 3-1 of Chapter 3 can be determined.

The core specific gravities calculated for the Configuration 2 wire diameters marked with an asterisk in Table 3-2 of Chapter 3 are given below in Table A-1 for 10 feet submergence and 20 feet submergence at towing speeds of 5 and 15 knots. A blank indicates that no SG_{core} greater than zero can be found for the given conditions.

TABLE A-1

SG_{core} For Various Wire Diameters, Depths of Submergence and Towing Speeds

d_2 (in.)	10 FEET SUBMERGENCE		20 FEET SUBMERGENCE	
	SG_{core} (V_n=5 knots)	SG_{core} (V_n=15 knots)	SG_{core} (V_n=5 knots)	SG_{core} (V_n=15 knots)
0.40	0.130	0.184	0.262	0.480
0.41	0.096	0.152	0.230	0.452
0.43	0.027	0.084	0.165	0.394
0.45	----	0.013	0.096	0.332
0.52	----	----	----	0.093